Acta Ophthalmologica

Effect of corneal incision features on anterior and posterior corneal astigmatism and higher-order aberrations after cataract surgery

Journal:	*Acta Ophthalmologica*
Manuscript ID	ACTA-20-06-1246.R1
Wiley - Manuscript type:	Original Article
Date Submitted by the Author:	20-Dec-2020
Complete List of Authors:	He, Qin; Zhejiang University School of Medicine First Affiliated Hospital, The Department of Ophthalmology Huang, Jiani; Zhejiang University School of Medicine First Affiliated Hospital, The Department of Ophthalmology He, Xiaoying; Zhejiang University School of Medicine First Affiliated Hospital, The Department of Ophthalmology Yu, Wangshu; Zhejiang University School of Medicine First Affiliated Hospital, The Department of Ophthalmology Yap, Maurice; The Hong Kong Polytechnic University School of Optometry Han, Wei; Zhejiang University School of Medicine First Affiliated Hospital, The Department of Ophthalmology
Keywords:	cataract surgery, clear corneal incision, optical coherence tomography, surgically induced astigmatism, higher-order aberrations

Title page

Effect of corneal incision features on anterior and posterior corneal astigmatism and higher-order aberrations after cataract surgery

Qin He, MD,[1]* Jiani Huang, MD,[1]* Xiaoying He, MD,[1] Wangshu Yu, MD,[1] Maurice Yap, PhD,[2] Wei Han, MD, PhD[1]†

[1]The Department of Ophthalmology, First Affiliated Hospital, School of Medicine, Zhejiang University, Hangzhou, Zhejiang, People's Republic of China

[2]School of Optometry, The Hong Kong Polytechnic University, Hong Kong, People's Republic of China

*These authors contributed equally to this work and should be regarded as co-first authors.

†Correspondence: Wei Han, the Department of Ophthalmology, First Affiliated Hospital, School of Medicine, Zhejiang University, 79 Qingchun Road, Hangzhou, Zhejiang 310003, China; E-mail: hanweidr@hotmail.com; Tel: 86-571-87236788; Fax: 86-571-87214128.

Abstract

Purpose: To evaluate the influence of 2.2 mm clear corneal incision (CCI) features in surgically induced astigmatism (SIA) and higher-order aberrations (HOAs) after cataract surgery.

Methods: Right eyes of 92 subjects receiving 2.2 mm incision cataract surgery were involved. 38 eyes were categorized as the intact incision group and 54 eyes were the defective incision group. Pre- and post-operative (1 month and 6 months) corneal astigmatism and HOAs on anterior and posterior corneal surfaces, corneal volume and corneal thickness (CT) were measured using Pentacam. The CCI features including incision length (IL), incision angles, distance from incision to central cornea (Dis-En/Ex), CT at incision site, were quantified using AS-OCT.

Results: The defective incision group showed shorter IL and larger incision angles [false discovery rate (FDR)-*P*<.05]. Changes in CT at incision site were more pronounced for the defective incision group (FDR-*P*<.05). Some SIA parameters were related to the certain specific CCI features, especially IL (FDR-*P*<.05). Both groups exhibited significant increased 6 mm posterior corneal tHOAs at 1 month (Bonferroni corrected-*P*<.01) and the defective incision group showed increased 6 mm posterior tHOAs at 6 months (Bonferroni corrected-*P*=.023). There were characteristic correlations between Zernike terms and CCI features including IL, CT, Dis-En/Ex, incision angles at 1 month, especially over 6 mm zone.

Conclusion: The CCI deformities can affect corneal recovery and induce more HOAs at 1 month postoperatively. Such effects became minor, but could persist until 6 months. The IL combined with Angle-En/Ex was important factor influencing CCI integrity and corneal optical quality.

Key Words

cataract surgery; clear corneal incision; optical coherence tomography; surgically induced astigmatism; higher-order aberrations

Introduction

Surgically induced astigmatism (SIA) after cataract surgery and its impact on corneal optical quality have been well-documented (Kim et al. 2016; Hayashi et al. 2018). However, apart from astigmatism, the higher-order aberrations (HOAs) are also important for visual quality (Namba et al. 2017; Hughes et al. 2020). Previous studies (von Sonnleithner et al. 2017; He et al. 2019) have observed significantly increased corneal HOAs after cataract surgery and its association with less than optimal visual quality (Namba et al. 2017). The surgical procedures, including clear corneal incision (CCI), phacoemulsification, stromal hydration and intraoperative flushing, may all affect corneal regularity on both the anterior and posterior corneal surfaces and consequently induce the HOAs.

Studies have demonstrated that a wider CCI causes more SIA and corneal HOAs changes (Denoyer et al. 2013; He et al. 2019), particularly at the posterior corneal surface (Ye et al. 2014; Hidaka et al. 2016; He et al. 2019). Apart from the incision width, the other fine architecture features of CCI, such as incision length (IL), deformities, distance to central cornea, may also be important for the degradation of postoperative corneal optical quality and deserving of further investigation. Since incomplete sealing frequently occurs at the internal wound site of CCI (Vasavada et al. 2013), one can speculate that the resulting corneal deformities could affect the corneal optical quality after cataract surgery.

With widespread adoption of sophisticated technologies like femtosecond laser, multifocal and toric IOLs, the quality of CCI have become a more prominent determinant for the visual quality outcome of the cataract surgery. However, to the best of our knowledge, there is no published study looking at the relationship between the CCI features and HOAs, especially on the posterior corneal surface.

The fine CCI features can be evaluated with the anterior segment optical coherence tomography (AS-OCT) (Nguyen & Chopra 2013; Lim 2015). Previous studies (Dupont-Monod et al. 2009; Xia et al. 2009; Can et al. 2011) evaluated corneal stromal edema around the CCI area on AS-OCT images. The CCI architecture deformities, including endothelial gap and Descemet membrane detachment (DMD), were also described using AS-OCT measurement (Calladine & Packard 2007; Xia et al. 2009; Chee et al. 2010; Can et al. 2011).

Therefore, the present work quantified the CCI architecture parameters, including IL, entry/exit angle, distance from incision to central cornea, corneal thickness (CT) at incision site, using AS-OCT in a group of patients receiving 2.2 mm incision phacoemulsification cataract surgery. The aim was to evaluate the role of the CCI architecture parameters in the postsurgical corneal SIA and HOAs at 1 month and 6 months after surgery. This work could contribute to the optimization of the CCI design and increase the accuracy or predictability of cataract surgery.

Methods

This study was performed at the Department of Ophthalmology, First Affiliated Hospital, Zhejiang University, Hangzhou, China. All participants provided informed consent. The study was approved by the hospital's ethics committee and performed in accordance with the tenets of the Declaration of Helsinki.

Patients with age-related cataract undergoing phacoemulsification and IOL implantation in the right eye were invited to join this study. Patients who met the following criteria were included: (1) right-eye cataract with nuclear opalescence of grade 2 to 4 according to the Lens Opacities Classification System III scale (Chylack et al. 1993), (2) preoperative corneal astigmatism less than 2.0 D, (3) axial length of 22.0 to 26.0 mm. The exclusion criteria were: (1) high myopia (worse than -6.0 D) or high hyperopia (greater than +3.0 D), (2) ocular surface disorders (severe dry eye, significant Meibomian gland dysfunction, entropion, trichiasis, ectropion), (3) corneal diseases, glaucoma, uveitis and retinal diseases, (4) history of ocular surgery or trauma, (5) systematic diseases (diabetic mellitus, thyroid disease, autoimmune disease), (6) significant surgery-related complications, (7) incomplete follow-up data.

All patients received a complete routine ocular examination within 2 weeks before surgery, including slit-lamp biomicroscopy, intra-ocular pressure measurement, computerized refraction, uncorrected distance visual acuity,

corrected distance visual acuity (CDVA), corneal endothelial cell count, ultra sound A and B scan, and fundus photography. The follow-up time of 1 month and 6 months was adopted.

AS-OCT assessments

The swept source AS-OCT (SS-1000 CASIA, Tomey Corp.) assessments were performed within 2 weeks preoperatively and at 1 month and 6 months postoperatively. The AS-OCT assessments were performed by one experienced examiner (H.Q.). Patients were required to blink before each measurement and keep their eyes open widely for sufficient exposure during assessment. For both pre- and postoperative assessments, radial scans taken at the corneal vertex were performed and patients were instructed to gaze at the fixation target. For postoperative CCI assessments, radial scans taken perpendicular to the CCI site were also performed and patients were instructed to look at the opposite side of the CCI. Each assessment was repeated until three usable measurements were acquired to ensure consistency.

Cross-sectional images of CCI were obtained and evaluated. The architectural deformities of CCI were categorized (Figure 1): (1) endothelial gap, (2) epithelial gap, (3) DMD and (4) wound misalignment. Incisions with either endothelial gap, epithelial gap, DMD or misalignment were grouped as defective incisions, the others were intact incisions. The following incision parameters were measured using the package caliper tool of Tomey

Measurement software (Tomey Corp.) and the abbreviations were used for easy reading (Figure 2): (1) IL, (2) angle between incision and corneal epithelium (incision entry angle, Angle-En), (3) angle between incision and corneal endothelium (incision exit angle, Angle-Ex), (4) CT at incision entry (CT-En), (5) CT at incision exit (CT-Ex), (6) the distance from incision entry to central cornea (incision entry distance, Dis-En), (7) the distance from incision exit to central cornea (incision exit distance, Dis-Ex). According to the CCI location, CT at the corresponding position before surgery was measured using the preoperative AS-OCT images. The discrepancy of CT at the CCI before and after surgery was calculated.

Pentacam assessments

The Pentacam assessments were completed as described in our previous work (He et al. 2019). Briefly, each patient received measurements preoperatively and postoperatively at 1 month and 6 months, and the following data were extracted: (1) keratometry of anterior and posterior cornea, (2) magnitude and meridian of anterior and posterior corneal astigmatism, (3) central corneal thickness (CCT), (4) corneal volume (CV), (5) coefficients of Zernike polynomials up to 4th order at central 4 mm and 6 mm diameter zones on total, anterior and posterior corneal surfaces. SIA vectors were calculated with the method described by Alpins (Alpins & Goggin 2004). The mean magnitudes of individual SIA vectors and the centroid values were reported.

The torque and flattening effect at the meridian of corneal incision were analyzed. The root-mean-square (RMS) of total HOAs (tHOAs) through the 3rd to 4th orders was calculated.

Surgical procedures

All the cataract surgery was performed by one experienced surgeon (H.W.), as described in our previous work (He et al. 2019). For all patients, a 2.2 mm CCI was created at the 11 o'clock meridian and a 0.6 mm subsidiary incision was made at 2 o'clock meridian using single-use steel blades. The surgery was performed using the Centurion System (Alcon, Inc.). An Akreos MI 60 IOL was implanted using the Hydroport PS27 injector system (Bausch + Lomb, Inc.). Intraoperative parameters including total operation time, U/S total time and cumulative dissipated energy were recorded.

Statistical Analysis

The sample size was calculated using PASS version 15.0. Based on a small-size retrospective pilot experiment, mean differences and standard deviations of IL (mean diff. = 0.18 mm, SD = 0.24 mm), SIA (mean diff. = 0.13 D, SD = 0.17 D) and HOAs (mean diff. = 0.025 μm, SD = 0.031 μm) were obtained for sample size calculation. The n of defective incision group was approximately 1.5 times that of intact incision group. Therefore, the group allocation index was set as 1.5. A sample size of 80 eyes (32 eyes for intact

incision group and 48 eyes for defective incision group) yielded 90% power with a type I error rate of 5%.

Statistical analysis was performed using SPSS software (version 22.0, IBM Corp.). A Kolmogorov-Smirnov test was used to test the normality of each data set. A Pearson chi-square test was used for categorical variables. The repeated-measures analysis of variance followed by Bonferroni post hoc test was applied to compare the preoperative data and postoperative data. For the within-group comparisons, a *P* value less than 0.05 was considered statistically significant.

The Mann-Whitney U test was performed for group-wise comparisons. The Spearman's correlation analysis was performed to test the correlation between the CCI architecture parameters and corneal SIA & HOAs. To solve the multiple-testing issue, the false discovery rate (FDR) was applied for the group-wise comparisons and correlation analyses (Benjamini & Hochberg 1995). An FDR level less than 0.05 was considered statistically significant.

Results

Totally 361 eyes (272 patients) received cataract surgery during study period. Only right eyes were assessed, and hence 149 left eyes were excluded. According to the inclusion and exclusion criteria, 129 eyes of 129 patients were included after preoperative examinations. Among them, 28 patients refused to participate, so that 101 eyes of 101 patients were enrolled in our observation.

Among the 101 patients, 9 patients failed to complete the follow-up. Finally, 92 eligible subjects (47 females and 45 males) were recruited. According to the CCI features assessed by AS-OCT at 1 month postoperatively, 38 eyes were categorized as the intact incision group and the remaining 54 eyes were the defective incision group.

The clinical information of the intact and defective groups is listed in Table 1. The baseline clinical data of the two groups were similar (Table 1 and Table S1).

(Insert Table 1 here)

CCI features assessments

The CCI features assessments at 1 month and 6 months postoperatively are listed in Table 2. For the defective incision group at 1 month postoperatively, 59.3% had endothelial gap, 13.0% had DMD and 33.3% had wound misalignment. No epithelial gap was observed. At 6 months, no DMD or epithelial gap was observed, but 5 (9.3%) eyes showed endothelial gap and 20 (37.0%) eyes showed wound misalignment for the defective incision group. The intact incision group had significant longer IL (P=.001, Mann-Whitney U test) and smaller incision angles (Angle-En, P=.000; Angle-Ex, P=.017). No difference was found between the two groups regarding the incision distances.

At 1 month, CV was significantly increased in both two groups (P<.05, repeated-measures analysis of variance followed by Bonferroni post hoc test).

At 6 months, no significant changes in CCT or CV were observed in comparisons with preoperative values for both groups. The changes in CCT and CV were similar between groups at each follow-up (*P*>.05). At 1 month, the defective group showed significant increase in CT-En and CT-Ex (*P*=.026, *P*<.001, respectively), while the intact group only showed significant increase in CT-Ex (*P*=.002). The changes in CT-Ex for the defective incision group were more pronounced (*P*<.001) at 1 month. At 6 months, CT-En and CT-Ex were similar to baseline for both groups, and no significant differences were observed between groups (Table 2).

Corneal SIA analysis

The SIA-related parameters on the anterior and posterior corneal surface showed no significant difference between the two groups after correction for multiple comparisons (Table 2).

(Insert Table 2 here)

Corneal tHOAs analysis (Figure 3)

After multiple comparisons correction, both groups showed no significant changes for total and anterior corneal tHOAs at postoperative 1 month and 6 months. The 4 mm posterior corneal tHOAs were slightly increased in the intact incision group (*P*=.032) at postoperative 1 month. The 6 mm posterior corneal tHOAs were increased in both groups (intact incision group, *P*=.007; defective

incision group, *P*<.001) at postoperative 1 month. At 6 months, statistically significant increase in the posterior corneal tHOAs over the 6 mm zone were only observed for the defective incision group (*P*=.023).

Corneal individual Zernike HOAs analysis

4 mm analytical zone (Figure 4). For the total cornea, the spherical aberration (SA) was significantly decreased (negative shift) in the two groups (*P*<.05), whereas significant changes in Z(3, -3) and Z(3, 3) terms were only present in the defective incision group (*P*<.05) at 1 month. For the anterior corneal surface, significant changes in SA, Z(3, -3) and Z(3, 3) were only present in the defective incision group (*P*<.05) at 1 month. For the posterior corneal surface, significant changes in Z(3, 3) terms were found in the defective incision group (*P*=.038) at 1 month. No changes in individual Zernike terms were observed at 6 months.

6 mm analytical zone (Figure 5). For the total cornea, Z(3,-1) showed significant negative shift in both groups at 1 month and 6 months postoperatively (*P*<.05). The SA decreased in both groups at postoperative 1 month (*P*<.001). At 6 months, the SA in defective incision group still had significant difference compared with the preoperative value (*P*=.005). Significant changes in Z(3, -3) and Z(3, 3) terms were only found in the defective incision group (*P*<.001). Z(4, 4) was significantly increased in both groups (*P*<.001) at 1 month. For the anterior corneal surface, the SA was significantly

decreased in both two groups (*P*<.001) at 1 month. Significant changes in Z(3, -3), Z(3, -1) and Z(3, 3) were found in the defective incision group (*P*<.001) at 1 month. Z(4, 4) was significantly increased in the two groups (*P*<.01) at 1 month. No changes in anterior corneal Zernike terms were observed at 6 months. For the posterior corneal surface, significant changes in SA, Z(3, -1), Z(3, 3), and Z(4, 4) were found for the defective incision group (*P*<.01) at 1 month. Changes in SA and Z(3, -1) were also observed at 6 months for defective incision group (*P*<.05). The intact incision group presented significant changes in Z(3,-1) and Z(4,-4) at postoperative 1 month (*P*<.01).

Correlation analysis between SIA and CCI features (Table 3)

With an FDR level of 0.05, the cutoff for significant correlation between SIA and CCI features was 0.0033. When 1 month postoperatively, for the intact incision group, the anterior corneal SIA torque was positively correlated with CT-En (*P*<.0033, Spearman's correlation analysis), while the anterior corneal SIA flattening effect showed positive correlation with the CCT and CV variations (*P*<.0033). The posterior surface SIA flattening and absolute torque showed weak positive correlation with incision angles and CT-Ex respectively (*P*<.0033). For the defective incision group 1 month postoperatively, the anterior corneal SIA was significantly correlated to IL and Angle-En (*P*<.0033). The posterior surface flattening effect was positively correlated to IL and negatively correlated to Dis-Ex (*P*<.0033). The posterior torque showed negative correlation with IL

and positive correlation with Angle-Ex (*P*<.0033).

At 6 months postoperatively, no significant correlation between SIA and CCI features was found for the intact incision group. For the defective incision group, IL still showed correlation with the anterior corneal SIA magnitude and torque and posterior corneal flattening (*P*< .0033). The Angle-En was correlated with the anterior surface SIA magnitude and Angle-Ex was correlated with posterior surface torque (*P*< .0033).

(Insert Table 3 here)

Correlation analysis between HOAs and CCI features

4 mm analytical zone (Table 4). With an FDR level of 0.05, the cutoff for significant correlation between 4 mm corneal HOAs and CCI features was 0.0025. For the intact incision group at 1 month postoperatively, CCT showed significant negative correlation with the posterior surface vertical coma (*P*<.0025). CT-Ex had close negative correlation with the posterior vertical coma and SA (*P*<.0025). IL was significantly negatively correlated to the total corneal vertical coma (*P*<.0025), while Angle-En had positive correlation with total corneal vertical coma and vertical trefoil (*P*<.0025). For the defective incision group, both CT-En and CT-Ex showed correlation with several Zernike aberrations, including the tHOAs, vertical coma, oblique trefoil and SA (*P*<.0025). IL was mainly negatively correlated to the total and anterior vertical coma (*P*<.0025). Angle-En presented positive correlation with the total and

anterior vertical coma (*P*<.0025), whereas Angle-Ex was positively correlated to the posterior oblique trefoil (*P*<.0025). The Dis-Ex had significant positive correlation with the posterior oblique trefoil (*P*<.0025).

(Insert Table 4 here)

6 mm analytical zone (Table 5). With an FDR level of 0.05, the cutoff for significant correlation between 6 mm corneal HOAs and CCI features was 0.0091. There were more HOAs parameters that significantly correlated with CCI features considering the 6 mm analytical zone than the 4 mm analytical zone. For the intact incision group 1 month postoperatively, CCT showed negative correlation with the posterior oblique trefoil (*P*<.0091), while CV was negatively correlated to the anterior surface SA and posterior oblique trefoil (*P*<.0091). Significant correlation between CT-En and the anterior surface tHOAs and vertical/horizontal coma changes was observed, whereas CT-Ex was strongly correlated to the anterior and posterior Zernike terms (*P*<.0091). IL was positively correlated to the posterior surface tHOAs and negatively correlated to the total vertical trefoil (*P*<.0091). Angle-En exhibited negative correlation with the total and anterior corneal tHOAs, and positive correlation with total and anterior corneal vertical coma and trefoil terms (*P*<.0091). There was obvious positive correlation between Dis-En and the total and anterior vertical coma, while Dis-Ex was positively correlated to the total, anterior and posterior vertical coma and the total SA (*P*<.0091). For the defective incision group, significant negative correlation of CV with the total and anterior vertical

coma was observed (*P*<.0091). CT-En and CT-Ex were negatively correlated to vertical coma (*P*<.0091) and CT-Ex was also negatively correlated to the total and anterior oblique trefoil and the posterior SA (*P*<.0091). IL presented correlation with the posterior tHOAs as well as the total and anterior vertical trefoil and horizontal coma (*P*<.0091). Angle-Ex was correlated to the total and anterior surface coma and posterior surface oblique trefoil (*P*<.0091). Correlation of Dis-En with tHOAs, total and anterior surface oblique trefoil and posterior surface SA reached significance (*P*<.0091), while Dis-Ex was negatively correlated to posterior tHOAs, and positively correlated to total and anterior oblique trefoil and the posterior vertical coma (*P*<.0091).

(Insert Table 5 here)

Discussion

CCI features analysis

At 1 month postoperatively, approximately 60% of patients exhibited defective incision features of endothelial gap, DMD or wound misalignment, indicating a prolonged wound healing (Figure 1). Previous studies have reported a range of incidences for patients who had defective incisions. This might be due to the discrepancies in surgical techniques, including femtosecond laser-created CCI (Alio et al. 2013; Grewal & Basti 2014; Chaves et al. 2019), incision width (Li et al. 2011; Li et al. 2018), stromal hydration (Fukuda et al. 2011; Bang et al. 2015), postoperative drug usage (Choi et al.

2016) and measuring principles.

The frequency of the DMD and wound misalignment at 1 month was similar to previous studies (Wang et al. 2012; Li et al. 2018; Rodrigues et al. 2019). At 6 months postoperatively, the features of defective CCI disappeared in most subjects of the defective incision group, while some subjects still showed wound misalignment (37%) and endothelial gap (9%) (Table 2). It was noticeable that at 6 months, the frequency of endothelial gap and DMD significantly declined, whereas the frequency of wound misalignment was slightly increased, indicating the long-term existence of wound misalignment as reported by previous studies (Choi et al. 2016; Li et al. 2018). Wound misalignment was associated with collagen deposits and incision remodeling (Li et al. 2018). The increased incidence of wound misalignment might be due to the healing effect of incisions with endothelial gap and DMD. The changing profile of endothelial gap, DMD and wound misalignment from 1 month to 6 months demonstrated the recovering and remodeling process of CCI.

Our data also revealed that the endothelial gap was much more common than the epithelial gap (Vasavada et al. 2013; Lee et al. 2014; Rodrigues et al. 2019). This may be due to the rapid healing of epithelium side compared with the endothelium side which was directly exposed to the inflammatory environment in aqueous humor. This further supported our previous finding that the changes in the posterior corneal HOAs were more pronounced after surgery (He et al. 2019).

The defective incision group had significantly shorter incision length and larger incision entry/exit angles, suggesting the shorter incision is more likely to be associated with the occurrence of the incision deformities. Hayashi et al. (Hayashi et al. 2018) also found a higher rate of DMD in short CCIs. The longer incisions require less hydration sealing and help incision healing (Fine et al. 2007), but may increase the chance of tear during the handpiece maneuver and IOL injection. In this study, we chose the 1.8 mm MI 60 IOL to minimize the influence of incision tear at the IOL implantation step. Our data suggests that longer incisions with smaller angles were beneficial to the incision integrity.

The changes in CV or CT indicated manifest cornea edema was present until 1 month postoperatively, which was similar to the previous studies (Li et al. 2011; Li et al. 2018). The increasing CT-Ex in both groups at 1 month demonstrated the retarded healing of the endothelium surface. Moreover, the retarded dissipation of cornea edema in the defective incision suggested the influence of incision deformities in the corneal wound healing (Table 2). At 6 months, CV and CT of both two groups returned to baseline level, suggesting the dissipation of corneal edema at both central cornea and CCI sites.

SIA and CCI features

Among the SIA indices, no significant differences between the defective and intact incision groups were observed at 1 month and 6 months postoperatively (FDR-*P*>.05) (Table 2). The results indicated the little impact of

CCI's integrity on SIA, as the 2.2 mm incision was thought not to cause significant SIA (Wang et al. 2009).

For the intact incision, some CCI features (CCT, CV and CT-En) showed correlation with the anterior surface flattening effect and torque at 1 month, but no significant correlation was observed at 6 months, indicating that the impact of corneal edema on the anterior surface SIA persisted until 1 month and declined at 6 months due to the dissipation of edema. For the defective incision, IL seemed to be the most important parameter influencing SIA. The IL showed positive correlation with the SIA magnitude at postoperative 1 month and 6 months. It was noticeable that the IL always exhibited reverse *r* values (positive correlation) when compared with the incision angles (negative correlation). Our data suggested that longer CCI coupled with smaller incision angles might cause more SIA on both anterior and posterior surfaces, especially in the defective incision group (Table 3).

Ferreira et al.(Ferreira et al. 2018) found less SIA in the femtosecond laser created incision than the manually 2.4 mm incisions. Zhu et al.(Zhu et al. 2017) found significant correlation between the SIA and distance from the incision entry to central cornea. Choi et al.'s work standardized the CCI deformities by wound deformity scoring and found positive correlations between SIA and wound instability (Choi et al. 2016). Our results were in agreement with the previous studies (Wilczynski et al. 2016; Hayashi et al. 2018; Sonmez & Karaca 2018) and we further evaluated the correlation between the CCI features and

corneal SIA on the anterior and posterior surfaces at 1 and 6 months postoperatively.

Total HOAs and CCI features

There are few studies regarding the relation between the CCI architecture features and corneal HOAs. Alio et al.(Alio et al. 2013) described the morphological changes of CCI after the femtosecond laser-assisted cataract surgery and found no significant changes in the corneal HOAs. Only slight increase of posterior corneal tHOAs over 4 mm zone was observed in the intact incision group (*P*=.032), indicating that the 4 mm tHOAs were less affected (Figure 3A). The changes in the 6 mm corneal tHOAs were more pronounced. Mild increase of the total corneal tHOAs over 6 mm zone at 1 month was observed in the defective incision group (*P*=.084), while the posterior corneal tHOAs changes over 6 mm zone were significant for both groups at 1 month, but at 6 months, the significance level was only observed in the defective incision group (Figure 3B). These results indicated the influence of incision deformities in the mid-peripheral and posterior corneal tHOAs.

The more pronounced and longer-standing posterior HOAs changes suggested the importance of the posterior corneal surface for the optical quality postoperatively. It is reasonable to speculate that changes in total and posterior corneal HOAs at 1 month were associated with significant corneal edema at central cornea and incision site. However, changes in posterior corneal HOAs

at 6 months ought to be related to the wound deformities like misalignment rather than corneal edema, as corneal edema should have dissipated at 6 months. In our subjects, the wound misalignment always occurred at incision exit, hence the posterior corneal HOAs were apt to be affected (Figure 3).

Individual HOAs and CCI features

Previous studies have found the changes in trefoil after surgery (Tong et al. 2008; Can et al. 2012; Yu et al. 2016). We found remarkable changes in vertical and oblique trefoil terms over the 4 mm and 6 mm zones in the defective incision group at 1 month. The CCI deformities in early postoperative stage might alter the corneal contour and induce more trefoil changes, as no evident changes in trefoil were found in the intact incision group. At late stage of 6 months postoperatively, no such significant changes were observed. The negative shift of SA in both incisions can be ascribed to the effect of corneal flattening due to the surgically induced stroma edema in the mid-peripheral corneal zone at 1 month. At 6 months, the changes in posterior SA over 6 mm zone were still observed in the defective incision group, indicating a long-term effect of CCI on posterior SA. Similarly, the 6 mm zone vertical coma on the total and posterior surfaces also showed negative shift for both incision groups. The vertical coma value is generally positive, due to the steeper contour of upper corneal zone compared with the lower corneal zone. The negative shift of vertical coma can also be ascribed to the superiorly located CCI (Song et al. 2015), which mainly

caused corneal edema and flattening of the corneal curvature in the upper zone. Such changes persisted until 6 months in our subjects. Besides, no evident changes in horizontal coma also support this point (Figures 4 and 5).

According to the HOAs analysis described above, the typical Zernike terms including coma, trefoil and SA were selected for the correlation analysis in order to evaluate the potential role of the CCI parameters in the corneal HOAs changes at postoperative 1 month. The correlation results between CCI features and HOAs at 6 months became much less significant and exhibited the random effects (data not shown), indicating the diminished significant impact of corneal incision on the HOAs. In general, the 4 mm HOAs showed less significant correlation with the CCI parameters than the 6 mm HOAs, suggesting less effect of CCI features on central optical quality. These results coincided with the observation that no significant difference in the postoperative central vision (CDVA) between the two groups (Table 1).

The vertical coma showed strong correlation with multiple CCI features, especially the CT, IL and incision angles. As described above, the superior CCI caused the asymmetrical cornea contour changes along the vertical meridian, hence the vertical coma was associated with the specific relevant CCI parameters. The 6 mm vertical coma was significantly associated with the Dis-En and Dis-Ex for the intact incision, but was less affected by Dis-En and Dis-Ex for the defective incision (Tables 4 and 5). For defective incision group, the vertical coma may be affected by other factors including corneal edema,

incision gap and DMD. These factors may have stronger effect in coma changes in cases of defective incisions.

Similar to SIA, the corneal tHOAs changes were positively correlated with IL and negatively correlated with incision angles. A longer IL tends to be more intact and well-sealing than a shorter one (Fine et al. 2007), but can enlarge the incision area and degrade the corneal optical quality. The shorter IL, coupled with larger incision angles, helps to reduce the HOAs or SIA. However, it was noticeable that the mean IL in the defective incision group (1.42±0.19 mm) was significantly shorter than that in the intact incision group (1.56±0.22 mm). Except for the risk of leakage, a short IL requires more hydration sealing and was more likely to cause incisions deformities and stromal edema at incision site, which were related to higher corneal HOAs and SIA as mentioned above (Tables 2, 3 and Figure 3). Thus, the IL has the dual effect on postoperative corneal HOAs and SIA.

The Dis-En and Dis-Ex are less important for the central 4 mm HOAs, but can influence the 6 mm HOAs changes especially in defective incision group (Table 5). In this study, the superiorly located incisions (at 11 o'clock meridian) were nearer to the cornea centroid and the effects on corneal optical quality should be more prominent when compared with the temporal incisions. Further investigations are necessary to determine the optimal incision parameters such as IL and CCI location.

Taken together, this study evaluated the CCI features after 2.2 mm incision

cataract surgery and found that the CCI deformities induced more postoperative corneal HOAs changes. Our results indicated that IL combined with Angle-En/Ex was closely related to the CCI integrity and had significant effects on the SIA and corneal HOAs changes at 1 month. At 6 months postoperatively, the effects of CCI were still present, although became obviously minor. Future studies involving more standardized parameters, including bi- or tri-planar CCI created by femtosecond laser, multiple CCI sizes and positions, would be clinically useful.

Acknowledgments

This study was supported by the National Natural Science Foundation of China (No. 81670842) and the Natural Science Foundation of Zhejiang Province (No. LQ20H120006). All authors declared no conflict of interest.

References

Alio JL, Abdou AA, Soria F, Javaloy J, Fernandez-Buenaga R, Nagy ZZ & Filkorn T (2013): Femtosecond laser cataract incision morphology and corneal higher-order aberration analysis. J Refract Surg **29**: 590-595.

Alpins NA & Goggin M (2004): Practical astigmatism analysis for refractive outcomes in cataract and refractive surgery. Surv Ophthalmol **49**: 109-122.

Bang JW, Lee JH, Kim JH & Lee DH (2015): Structural analysis of different incision sizes and stromal hydration in cataract surgery using anterior

segment optical coherence tomography. Korean J Ophthalmol **29**: 23-30.

Benjamini Y & Hochberg Y (1995): Controlling the false discovery rate: a practical and powerful approach to multiple testing. J R Stat Soc Ser B Methodol **57**: 289-300.

Calladine D & Packard R (2007): Clear corneal incision architecture in the immediate postoperative period evaluated using optical coherence tomography. J Cataract Refract Surg **33**: 1429–1435

Can I, Bayhan HA, Celik H & Bostanci Ceran B (2011): Anterior segment optical coherence tomography evaluation and comparison of main clear corneal incisions in microcoaxial and biaxial cataract surgery. J Cataract Refract Surg **37**: 490-500.

Can I, Bayhan HA, Celik H & Ceran BB (2012): Comparison of corneal aberrations after biaxial microincision and microcoaxial cataract surgeries: a prospective study. Curr Eye Res **37**: 18-24.

Chaves MAPD, de Medeiros AL, Vilar CMC, et al. (2019): Architecture evaluation of the main clear corneal incisions in femtosecond laser-assisted cataract surgery by optical coherence tomography imaging. Clin Ophthalmol **13**: 365-372.

Chee SP, Ti SE, Lim L, Chan AS & Jap A (2010): Anterior segment optical coherence tomography evaluation of the integrity of clear corneal incisions: a comparison between 2.2-mm and 2.65-mm main incisions. Am J Ophthalmol **149**: 768-776.

Choi EY, Kang HG, Kim TI, Kim EK & Lee HK (2016): Effect of postoperative administration of nonsteroidal antiinflammatory drugs and steroids on the conformational changes in wound healing after cataract surgery. J Cataract Refract Surg **42**: 1804-1813.

Chylack LT Jr, Wolfe JK, Singer DM, et al. (1993): The Lens Opacities Classification System III. The Longitudinal Study of Cataract Study Group. Arch Ophthalmol **111**: 831-836.

Denoyer A, Ricaud X, Van Went C, Labbé A & Baudouin C (2013): Influence of corneal biomechanical properties on surgically induced astigmatism in cataract surgery. J Cataract Refract Surg **39**: 1204-1210.

Dupont-Monod S, Labbe A, Fayol N, Chassignol A, Bourges JL & Baudouin C (2009): In vivo architectural analysis of clear corneal incisions using anterior segment optical coherence tomography. J Cataract Refract Surg **35**: 444-450.

Ferreira TB, Ribeiro FJ, Pinheiro J, Ribeiro P & O'Neill JG (2018): Comparison of surgically induced astigmatism and morphologic features resulting from femtosecond laser and manual clear corneal incisions for cataract surgery. J Refract Surg **34**: 322-329.

Fine IH, Hoffman RS & Packer M (2007): Profile of clear corneal cataract incisions demonstrated by ocular coherence tomography. J Cataract Refract Surg **33**: 94-97.

Fukuda S, Kawana K, Yasuno Y & Oshika T (2011): Wound architecture of clear corneal incision with or without stromal hydration observed with 3-

dimensional optical coherence tomography. Am J Ophthalmol **151**: 413-419.

Grewal DS & Basti S (2014): Comparison of morphologic features of clear corneal incisions created with a femtosecond laser or a keratome. J Cataract Refract Surg **40**: 521-530.

Hayashi K, Sasaki H, Manabe SI & Hirata A (2018): Intraocular pressure and wound state immediately after long versus short clear corneal incision cataract surgery. Jpn J Ophthalmol **62**: 621-627.

Hayashi K, Yoshida M, Hirata A & Yoshimura K (2018): Changes in shape and astigmatism of total, anterior, and posterior cornea after long versus short clear corneal incision cataract surgery. J Cataract Refract Surg **44**: 39-49.

He Q, Huang J, Xu Y & Han W (2019): Changes in total, anterior, and posterior corneal surface higher-order aberrations after 1.8 mm incision and 2.8 mm incision cataract surgery. J Cataract Refract Surg **45**: 1135-1147.

Hidaka Y, Yamaguchi T, Saiki M, Dogru M, Tsubota K & Negishi K (2016): Changes in corneal aberrations after cataract surgery. Jpn J Ophthalmol **60**: 135-141.

Hughes RP, Vincent SJ, Read SA & Collins MJ (2020): Higher order aberrations, refractive error development and myopia control: a review. Clin Exp Optom **103**: 68-85.

Kim YJ, Knorz MC, Auffarth GU & Choi CY (2016): Change in anterior and posterior curvature after cataract surgery. J Refract Surg **32**: 754-759.

Lee H, Kim EK, Kim HS & Kim TI (2014): Fourier-domain optical coherence

tomography evaluation of clear corneal incision structure according to blade material. J Cataract Refract Surg **40**: 1615-1624.

Li SS, Misra SL, Wallace HB & McKelvie J (2018): Effect of phacoemulsification incision size on incision repair and remodeling: Optical coherence tomography assessment. J Cataract Refract Surg **44**: 1336-1343.

Li YJ, Kim HJ & Joo CK (2011): Early changes in corneal edema following torsional phacoemulsification using anterior segment optical coherence tomography and Scheimpflug photography. Jpn J Ophthalmol **55**: 196-204.

Lim S (2015): Clinical applications of anterior segment optical coherence tomography. J Ophthalmol **2015**: 605729.

Namba H, Kawasaki R, Sugano A, Murakami T, Nishitsuka K, Kato T, Kayama T & Yamashita H (2017): Age-related changes in ocular aberrations and the Yamagata study (Funagata). Cornea **36**: S34-S40.

Nguyen P & Chopra V (2013): Applications of optical coherence tomography in cataract surgery. Curr Opin Ophthalmol **24**: 47–52.

Rodrigues R, Santos MSD, Silver RE, Campos M & Gomes RL (2019): Corneal incision architecture: VICTUS femtosecond laser vs manual keratome. Clin Ophthalmol **13**: 147-152.

Song IS, Park JH, Park JH, Yoon SY, Kim JY, Kim MJ & Tchah H (2015): Corneal coma and trefoil changes associated with incision location in cataract surgery. J Cataract Refract Surg **41**: 2145-2151.

Sonmez S & Karaca C (2018): The effect of tunnel length and position on

postoperative corneal astigmatism: An optical coherence tomographic study. Eur J Ophthalmol: 1120672118805875.

Tong N, He JC, Lu F, Wang Q, Qu J & Zhao YE (2008): Changes in corneal wavefront aberrations in microincision and small-incision cataract surgery. J Cataract Refract Surg **34**: 2085-2090.

Vasavada V, Vasavada AR, Vasavada VA, Srivastava S, Gajjar DU & Mehta S (2013): Incision integrity and postoperative outcomes after microcoaxial phacoemulsification performed using 2 incision-dependent systems. J Cataract Refract Surg **39**: 563-571.

von Sonnleithner C, Pilger D, Homburg D, Brockmann T, Torun N & Bertelmann E (2017): Corneal higher-order aberrations after phacoemulsification: a comparison of 3 different incision sizes. Eur J Ophthalmol **27**: 402-406.

Wang J, Zhang EK, Fan WY, Ma JX & Zhao PF (2009): The effect of micro-incision and small-incision coaxial phaco-emulsification on corneal astigmatism. Clin Exp Ophthalmol **37**: 664-669.

Wang L, Dixit L, Weikert MP, Jenkins RB & Koch DD (2012): Healing changes in clear corneal cataract incisions evaluated using Fourier-domain optical coherence tomography. J Cataract Refract Surg **38**: 660-665.

Wilczynski M, Supady E, Wierzchowski T, Zdzieszynski M & Omulecki W (2016): The effect of corneal tunnel length in patients after standard phacoemulsification through a 2.75 mm incision on surgically induced astigmatism, corneal thickness and endothelial cell density. Klin Oczna **117**:

236-242.

Xia Y, Liu X, Luo L, Zeng Y, Cai X, Zeng M & Liu Y (2009): Early changes in clear cornea incision after phacoemulsification: an anterior segment optical coherence tomography study. Acta Ophthalmol **87**: 764-768.

Ye H, Zhang K, Yang J & Lu Y (2014): Changes of corneal higher-order aberrations after cataract surgery. Optom Vis Sci **91**: 1244-1250.

Yu YB, Zhu YN, Wang W, Zhang YD, Yu YH & Yao K (2016): A comparable study of clinical and optical outcomes after 1.8, 2.0 mm microcoaxial and 3.0 mm coaxial cataract surgery. Int J Ophthalmol **9**: 399-405.

Zhu S, Qu N, Wang W, Zhu Y, Shentu X, Chen P, Xu W & Yao K (2017): Morphologic features and surgically induced astigmatism of femtosecond laser versus manual clear corneal incisions. J Cataract Refract Surg **43**: 1430-1435.

Figure legends

Figure 1. Representative AS-OCT images of 2.2 mm clear corneal incisions showing intact architecture (top left), endothelial gap (top right), Descemet membrane detachment (bottom left) and wound misalignment (bottom right).

Figure 2. Assessments of CCI features on AS-OCT images (IL = incision length; Angle-Ex = angle between incision and corneal endothelium; Angle-En = angle between incision and corneal epithelium; CT-Ex = corneal thickness at incision exit; CT-En = corneal thickness at incision entry; Dis-Ex = the distance from incision exit to central cornea; Dis-En = the distance from incision entry to central cornea).

Figure 3. Total higher-order aberrations over the 4 mm (A) and 6 mm (B) analytical zones by group. The *P* value is shown when there is significant difference between preoperative data and postoperative data (pre = preoperative data; post = postoperative data; tHOAs = total higher-order aberrations).

Figure 4. Individual Zernike terms for total (A), anterior (B), and posterior (C) corneal surfaces over the 4 mm analytical zone by group. The *P* value is shown when there is significant difference between preoperative data and postoperative data (pre = preoperative data; post = postoperative data).

Figure 5. Individual Zernike terms for total (A), anterior (B), and posterior (C) corneal surfaces over the 6 mm analytical zone by group. The *P* value is shown when there is significant difference between preoperative data and postoperative data (pre = preoperative data; post = postoperative data).

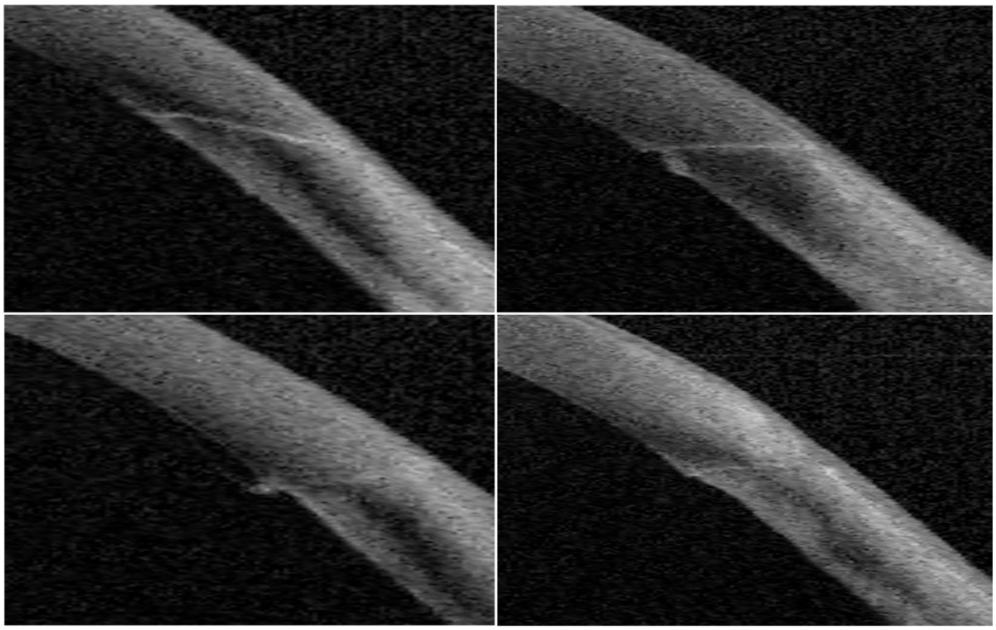

Figure 1. Representative AS-OCT images of 2.2 mm clear corneal incisions showing intact architecture (top left), endothelial gap (top right), Descemet membrane detachment (bottom left) and wound misalignment (bottom right).

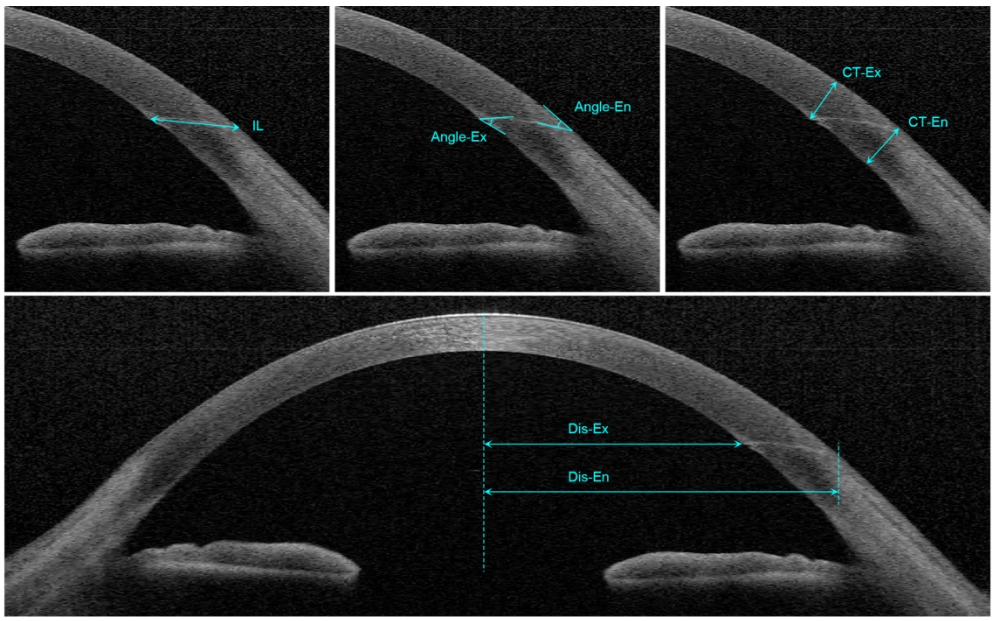

Figure 2. Assessments of CCI features on AS-OCT images (IL = incision length; Angle-Ex = angle between incision and corneal endothelium; Angle-En = angle between incision and corneal epithelium; CT-Ex = corneal thickness at incision exit; CT-En = corneal thickness at incision entry; Dis-Ex = the distance from incision exit to central cornea; Dis-En = the distance from incision entry to central cornea).

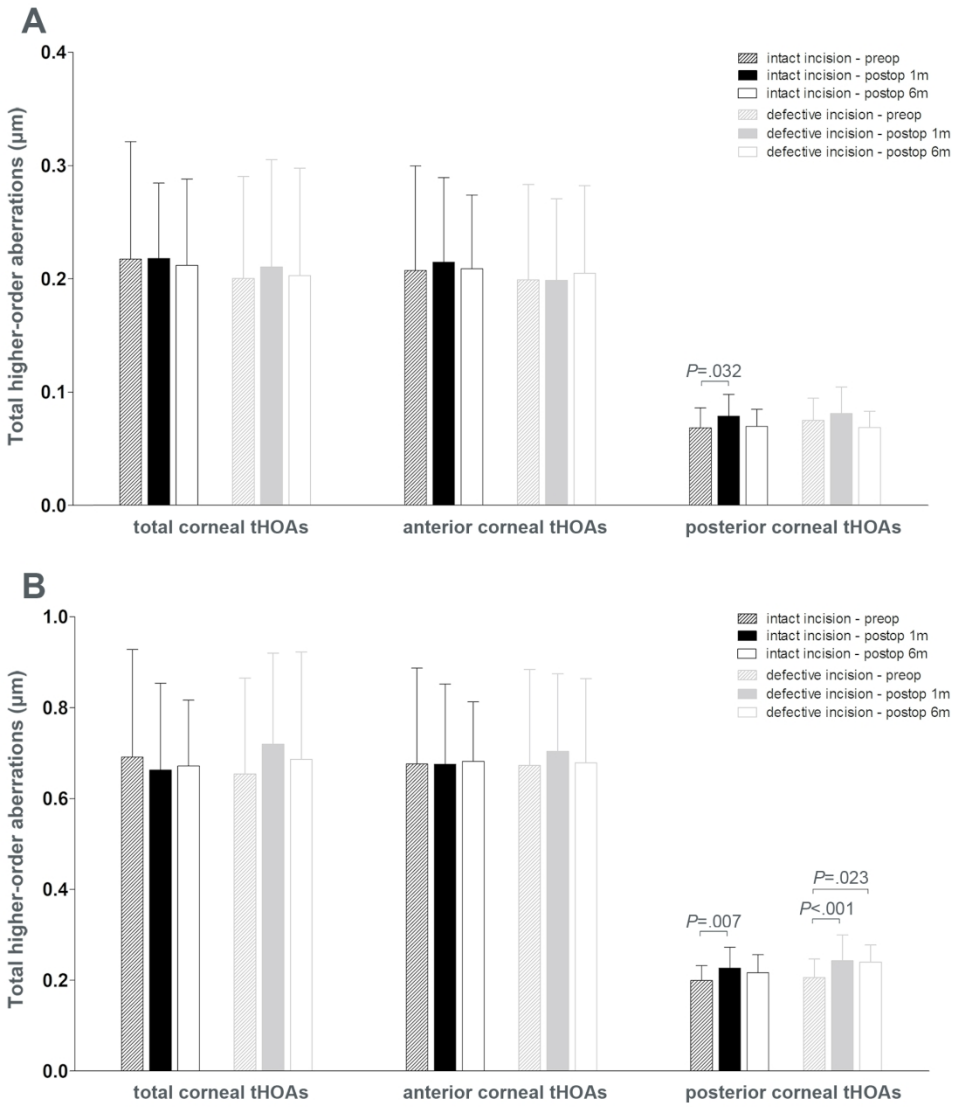

Figure 3. Total higher-order aberrations over the 4 mm (A) and 6 mm (B) analytical zones by group. The *P* value is shown when there is significant difference between preoperative data and postoperative data (pre = preoperative data; post = postoperative data; tHOAs = total higher-order aberrations).

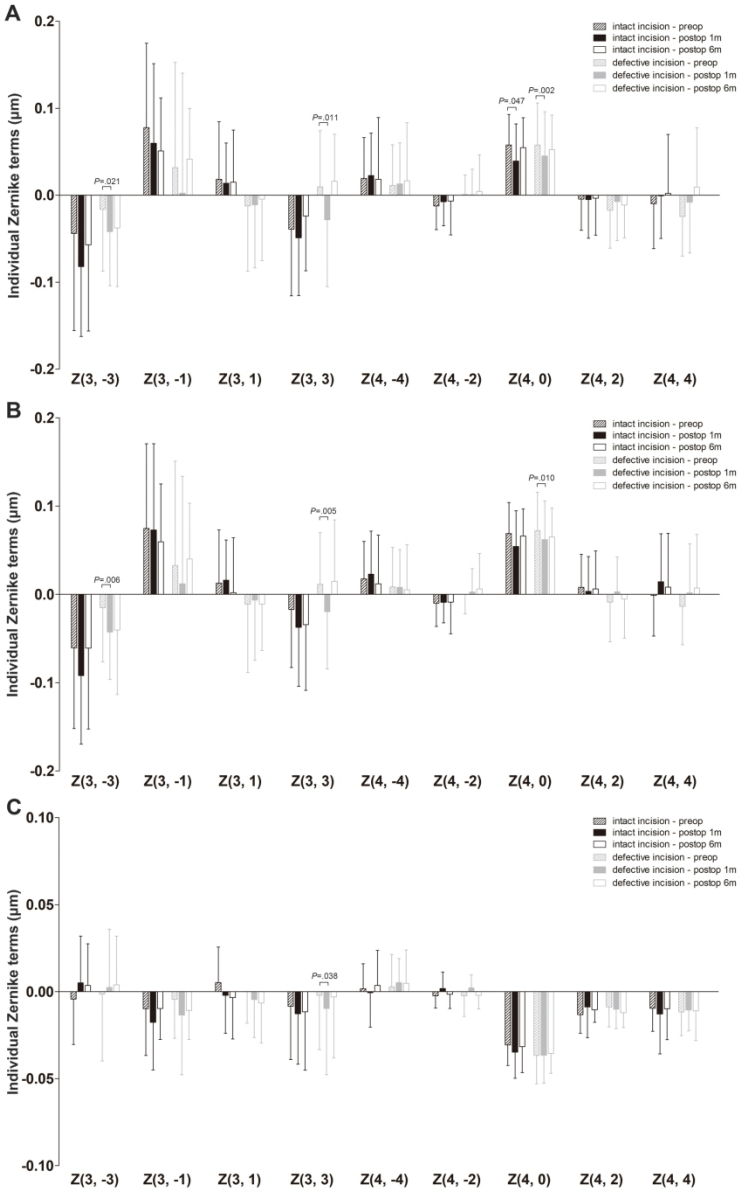

Figure 4. Individual Zernike terms for total (A), anterior (B), and posterior (C) corneal surfaces over the 4 mm analytical zone by group. The *P* value is shown when there is significant difference between preoperative data and postoperative data (pre = preoperative data; post = postoperative data).

177x272mm (300 x 300 DPI)

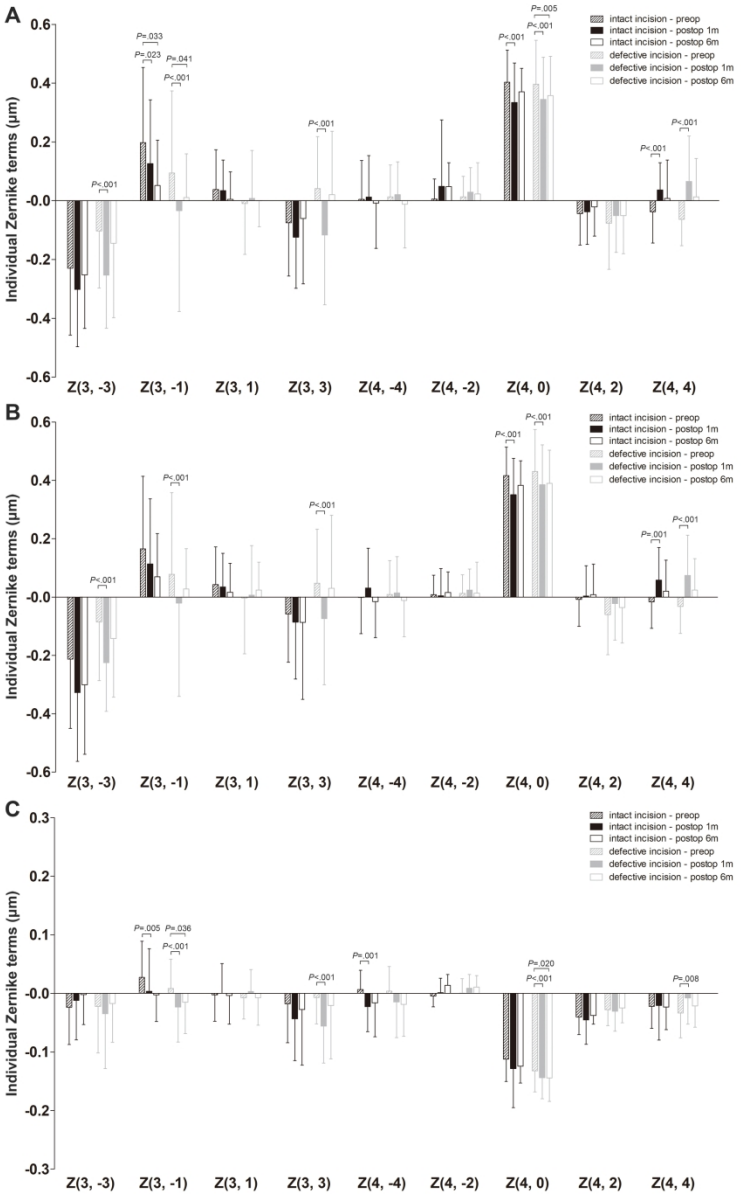

Figure 5. Individual Zernike terms for total (A), anterior (B), and posterior (C) corneal surfaces over the 6 mm analytical zone by group. The *P* value is shown when there is significant difference between preoperative data and postoperative data (pre = preoperative data; post = postoperative data).

177x272mm (300 x 300 DPI)

Table 1 Patient baseline characteristics and surgical data by CCI integrity.

Parameter	Intact incision	Defective incision	*P*
Eyes (n)	38	54	
Sex, n (%)			.549
Male	20 (52.6)	25 (46.3)	
Female	18 (47.4)	29 (53.7)	
Age (y)	71.1±9.1	68.9±10.5	.175
MRSE (D)	-2.07±2.48	-1.80±2.90	.359
CDVA (logMAR)			
Preoperative	0.54±0.23	0.61±0.28	.323
Postoperative	0.08±0.10	0.13±0.23	.274
Corneal optical data			
Anterior cornea			
Kf (D)	43.92±1.18	43.52±1.56	.204
Ks (D)	44.61±1.19	44.20±1.71	.092
Astigmatism magnitude (D)	0.69±0.41	0.69±0.49	.750
Astigmatism meridian (°)	124.5±53.4	114.5±54.4	.210
Posterior cornea			
Kf (D)	-6.33±0.27	-6.23±0.24	.075
Ks (D)	-6.56±0.24	-6.49±0.25	.268
Astigmatism magnitude (D)	0.23±0.14	0.26±0.15	.395
Astigmatism meridian (°)	93.0±18.9	92.6±24.6	.949
Nuclear opalescence*	2.78±0.62	2.99±0.79	.179
Total operation time (min)	11.56±2.79	12.23±2.66	.234
U/S total time (s)	58.07±6.83	59.74±9.25	.375
Cumulative dissipated energy	6.43±2.85	6.94±3.18	.359

CCI = clear corneal incision; MRSE = mean refractive spherical equivalent; CDVA = corrected distance visual acuity; logMAR = logarithm of the minimum angle of resolution; Kf = flat keratometry; Ks = steep keratometry

Means ± SD

*According to Lens Opacities Classification System III scale

Table 2 Clinical assessments by CCI integrity.

Parameter	Intact incision (n=38)	Defective incision (n=54)	*P*
CCI features assessments			
Endothelial gap, n (%)			
Postoperative 1 month	0 (0)	32 (59.3)	NA
Postoperative 6 months	0 (0)	5 (9.3)	NA
Epithelial gap, n (%)			
Postoperative 1 month	0 (0)	0 (0)	NA
Postoperative 6 months	0 (0)	0 (0)	NA
DMD, n (%)			
Postoperative 1 month	0 (0)	7 (13.0)	NA
Postoperative 6 months	0 (0)	0 (0)	NA
Wound misalignment, n (%)			
Postoperative 1 month	0 (0)	18 (33.3)	NA
Postoperative 6 months	0 (0)	20 (37.0)	NA
Incision width (mm)	2.2	2.2	NA
IL (mm)	1.56±0.22	1.42±0.19	.001[a]
Angle-En (°)	30.20±3.88	35.01±6.57	.000[a]
Angle-Ex (°)	31.58±7.26	35.74±8.54	.017[a]
Dis-En (mm)	5.40±0.49	5.24±0.37	.295
Dis-Ex (mm)	3.84±0.53	3.79±0.40	.912
Corneal thickness assessments			
CCT (μm)			
Preoperative	533.9±33.9	533.1±28.4	.801
Postoperative 1 month	540.9±38.1	540.3±25.9	.743
Postoperative 6 months	535.4±34.2	536.7±27.3	.840
CV (mm^3)			
Preoperative	59.08±3.90	59.33±3.51	.544
Postoperative 1 month	60.17±3.95*	60.30±2.91*	.801
Postoperative 6 months	59.28±4.01	59.72±3.71	.585
CT-En (μm)			
Preoperative	777.8±62.2	759.1±47.8	.312
Postoperative 1 month	787.9±52.9	777.8±54.1*	.495
Postoperative 6 months	779.3±59.3	765.3±45.3	.203
CT-Ex (μm)			
Preoperative	651.5±36.7	660.8±30.3	.724
Postoperative 1 month	693.9±37.8*	747.3±60.7*	.000[b]
Postoperative 6 months	658.6±34.5	673.1±41.2	.079

Corneal SIA assessments (postop 1m)[c]			
Anterior cornea			
SIA magnitude (D)	0.31±0.19	0.47±0.46	.165
Centroid SIA (magnitude @ axis)	0.18 @ 47.9	0.27 @ 80.0	NA
Flattening effect (D)	-0.15±0.24	-0.04±0.27	.142
Torque (D)	-0.11±0.20	-0.27±0.54	.301
Absolute torque (D)	0.19±0.12	0.40±0.45	.014
Posterior cornea			
SIA magnitude (D)	0.13±0.06	0.14±0.11	.743
Centroid SIA (magnitude @ axis)	0.06 @110.5	0.03 @ 73.7	NA
Flattening effect (D)	0.05±0.12	-0.00±0.14	.078
Torque (D)	-0.02±0.06	-0.03±0.10	.631
Absolute torque (D)	0.05±0.04	0.08±0.07	.216
Corneal SIA assessments (postop 6m)[c]			
Anterior cornea			
SIA magnitude (D)	0.31±0.20	0.37±0.23	.197
Centroid SIA (magnitude @ axis)	0.16 @ 59.2	0.20 @ 74.9	NA
Flattening effect (D)	-0.12±0.24	-0.05±0.18	.113
Torque (D)	-0.11±0.25	-0.19±0.33	.210
Absolute torque (D)	0.20±0.16	0.29±0.20	.023
Posterior cornea			
SIA magnitude (D)	0.13±0.07	0.14±0.09	.567
Centroid SIA (magnitude @ axis)	0.05 @ 104.5	0.03 @ 85.3	NA
Flattening effect (D)	0.04±0.12	0.02±0.11	.410
Torque (D)	-0.02±0.10	-0.01±0.08	.596
Absolute torque (D)	0.04±0.06	0.05±0.05	.387

CCI = clear corneal incision; NA = not applicable; DMD = Descemet membrane detachment; IL = incision length; Angle-En = angle between incision and corneal epithelium; Angle-Ex = angle between incision and corneal endothelium; Dis-En = the distance from incision entry to central cornea; Dis-Ex = the distance from incision exit to central cornea; CCT = central corneal thickness; CV = corneal volume; CT-En = corneal thickness at incision entry; CT-Ex = corneal thickness at incision exit; SIA = surgically induced astigmatism; postop = postoperative

Means ± SD

*Significant (P<.05) between the preoperative and postoperative data

[a]Significant (P<.03) after correction for multiple comparisons (n=5) based on false discovery rate (FDR)

[b]Significant (P<.0042) after correction for multiple comparisons (n=12) based on FDR

[c]No significant difference after correction for multiple comparisons (n=16) based on FDR

Table 3 Correlation analysis between corneal SIA and CCI features.

Postoperative 1 month	CCT	CV	CT-En	CT-Ex	IL	Angle-En	Angle-Ex	Dis-En	Dis-Ex
Intact incision group									
Anterior cornea									
SIA magnitude	-0.196	-0.226	-0.138	0.002	0.296	-0.315	-0.089	0.020	-0.053
Flattening	**0.571***	**0.666***	0.169	-0.049	-0.070	-0.101	0.218	0.303	0.307
Torque	0.104	0.004	**0.689***	0.205	0.139	0.205	-0.260	-0.357	-0.368
Absolute torque	0.017	0.147	-0.13	-0.092	0.219	-0.272	0.066	0.264	0.180
Posterior cornea									
SIA magnitude	-0.459	-0.185	0.033	0.084	0.075	0.365	0.158	-0.332	-0.307
Flattening	-0.131	-0.058	0.034	-0.358	-0.408	0.454	**0.632***	-0.187	-0.017
Torque	-0.104	-0.158	-0.244	0.267	0.333	-0.332	-0.222	-0.04	-0.126
Absolute torque	0.206	0.18	0.342	**0.673***	-0.275	**0.650***	0.136	-0.353	-0.215
Defective incision group									
Anterior cornea									
SIA magnitude	0.124	0.056	0.025	0.116	**0.690***	-0.434	-0.322	-0.045	-0.412
Flattening	-0.410	-0.440	-0.023	0.098	0.267	-0.207	0.025	-0.170	-0.269
Torque	-0.198	-0.153	-0.191	-0.192	**-0.609***	**0.491***	0.294	0.009	0.359
Absolute torque	0.131	0.057	0.025	0.112	**0.668***	-0.420	-0.307	-0.057	-0.412
Posterior cornea									
SIA magnitude	0.079	0.103	0.111	0.009	0.399	-0.211	-0.155	0.295	-0.007
Flattening	-0.053	-0.141	-0.168	-0.040	**0.556***	-0.383	-0.324	-0.219	**-0.475***
Torque	-0.149	-0.055	0.198	0.240	**-0.464***	0.331	**0.555***	-0.062	0.224
Absolute torque	0.158	0.135	0.092	-0.007	0.345	-0.188	-0.322	0.080	-0.176
Postoperative 6 months	CCT	CV	CT-En	CT-Ex	IL	Angle-En	Angle-Ex	Dis-En	Dis-Ex
Intact incision group									
Anterior cornea									
SIA magnitude	-0.235	-0.183	-0.128	0.005	0.301	-0.289	-0.077	0.132	-0.095

Flattening	0.269	0.311	0.184	-0.025	-0.056	-0.121	0.196	0.274	0.269
Torque	0.079	0.011	0.279	0.190	0.147	0.214	-0.232	-0.285	-0.317
Absolute torque	0.020	0.134	-0.112	-0.104	0.165	-0.267	0.122	0.298	0.203
Posterior cornea									
SIA magnitude	-0.294	-0.174	0.042	0.101	0.110	0.347	0.163	-0.319	-0.345
Flattening	-0.122	-0.044	0.053	-0.248	-0.307	0.310	0.523	-0.113	-0.026
Torque	-0.094	-0.134	-0.286	0.211	0.246	-0.214	-0.258	-0.064	-0.085
Absolute torque	0.212	0.208	0.244	0.342	-0.313	0.496	0.127	-0.276	-0.204
Defective incision group									
Anterior cornea									
SIA magnitude	0.175	0.063	0.017	0.121	**0.598***	-0.427	-0.375	-0.078	-0.376
Flattening	-0.263	-0.281	-0.046	0.074	0.277	-0.245	0.101	-0.194	-0.225
Torque	-0.244	-0.165	-0.153	-0.201	**-0.513***	0.398	0.309	0.027	0.293
Absolute torque	0.174	0.028	0.011	0.104	**0.534***	-0.347	-0.312	-0.069	-0.341
Posterior cornea									
SIA magnitude	0.084	0.118	0.107	0.012	0.312	-0.246	-0.163	0.270	-0.013
Flattening	-0.035	-0.137	-0.189	-0.011	**0.507***	-0.319	-0.331	-0.264	-0.391
Torque	-0.186	-0.079	0.211	0.266	-0.394	0.380	**0.485***	-0.115	0.178
Absolute torque	0.166	0.190	0.035	-0.024	0.327	-0.147	-0.295	0.071	-0.164

SIA = surgically induced astigmatism; CCI = clear corneal incision; CCT = central corneal thickness; CV = corneal volume; CT-En = corneal thickness at incision entry; CT-Ex = corneal thickness at incision exit; IL = incision length; Angle-En = angle between incision and corneal epithelium; Angle-Ex = angle between incision and corneal endothelium; Dis-En = the distance from incision entry to central cornea; Dis-Ex = the distance from incision exit to central cornea

*Significant (P<.0033) after correction for multiple testing (n=288) based on false discovery rate (FDR)

Table 4 Correlation analysis between corneal HOAs (4 mm zone) and CCI features.

	CCT	CV	CT-En	CT-Ex	IL	Angle-En	Angle-Ex	Dis-En	Dis-Ex
Intact incision group									
Total cornea									
Total HOAs	-0.021	-0.04	0.387	0.308	0.245	-0.189	-0.139	-0.125	0.039
Vertical trefoil	-0.059	-0.197	-0.381	-0.343	-0.358	**0.492***	0.319	0.259	-0.071
Vertical coma	-0.294	-0.094	-0.367	-0.408	**-0.638***	**0.513***	0.440	-0.04	0.072
Horizontal coma	-0.177	-0.109	0.081	-0.147	-0.206	-0.001	-0.072	0.093	0.032
Oblique trefoil	0.022	0.105	-0.414	-0.205	-0.243	0.327	0.286	0.266	-0.097
SA	0.201	0.259	0.099	-0.443	0.018	0.268	0.039	0.076	0.017
Anterior cornea									
Total HOAs	0.053	0.069	0.356	0.154	0.19	-0.149	-0.112	-0.247	-0.195
Vertical trefoil	-0.131	-0.239	-0.429	-0.046	-0.399	0.435	0.288	0.157	-0.06
Vertical coma	-0.083	-0.027	-0.132	-0.380	-0.252	0.423	0.285	0.144	0.216
Horizontal coma	-0.182	-0.072	-0.273	0.01	0.225	0.067	-0.085	0.127	0.043
Oblique trefoil	0.183	0.028	-0.413	-0.126	-0.135	0.101	0.091	0.123	0.169
SA	0.291	0.307	0.105	-0.386	0.07	0.312	0.013	0.062	-0.013
Posterior cornea									
Total HOAs	0.02	0.019	0.281	0.075	0.07	-0.235	-0.11	0.144	0.104
Vertical trefoil	0.217	0.086	-0.19	-0.138	-0.094	0.164	-0.115	-0.092	-0.09
Vertical coma	**-0.524***	-0.393	-0.033	**-0.575***	-0.141	0.239	0.245	0.154	0.276
Horizontal coma	-0.065	-0.13	-0.383	-0.223	0.031	0.138	0.022	0.057	0.017
Oblique trefoil	-0.202	-0.192	-0.067	-0.366	-0.025	0.074	-0.023	0.405	0.315
SA	-0.246	-0.074	0.08	**-0.486***	-0.161	-0.013	0.09	0.119	0.138
Defective incision group									
Total cornea									
Total HOAs	-0.07	0.229	**0.410***	0.07	-0.157	0.036	0.135	-0.196	-0.023
Vertical trefoil	0.101	0.039	-0.103	-0.041	0.012	0.368	-0.093	0.052	0.043

Vertical coma	-0.226	-0.141	-0.286	-0.349	**-0.391***	**0.462***	0.350	-0.109	0.131
Horizontal coma	-0.038	-0.111	-0.390	-0.128	0.127	-0.182	-0.048	0.093	0.05
Oblique trefoil	0.048	0.226	-0.368	-0.252	0.194	-0.01	-0.252	-0.262	-0.25
SA	0.224	0.193	-0.155	-0.331	0.151	-0.2	-0.181	-0.187	-0.254
Anterior cornea									
Total HOAs	-0.132	0.099	0.241	0.039	-0.133	-0.052	0.118	-0.227	-0.067
Vertical trefoil	-0.001	0.057	0.025	0.155	0.066	0.352	0.154	0.092	0.037
Vertical coma	-0.224	-0.216	-0.288	**-0.421***	**-0.468***	**0.521***	0.379	-0.003	0.224
Horizontal coma	-0.062	-0.111	-0.365	-0.09	0.132	-0.229	-0.061	0.055	0.033
Oblique trefoil	0.027	0.134	**-0.430***	-0.374	0.06	0.114	0.299	-0.108	-0.074
SA	0.103	0.022	-0.193	-0.288	-0.232	0.241	0.341	-0.052	-0.196
Posterior cornea									
Total HOAs	0.282	0.310	0.188	0.251	0.239	-0.171	-0.149	-0.066	-0.069
Vertical trefoil	0.08	-0.066	-0.213	0	-0.045	-0.071	0.054	0.005	0.053
Vertical coma	-0.123	-0.139	-0.182	-0.278	-0.027	0.116	0.12	0.362	-0.177
Horizontal coma	0.183	0.023	-0.284	-0.198	-0.042	0.106	0.085	0.067	0.019
Oblique trefoil	0.061	-0.258	-0.099	0.057	-0.321	0.206	**0.493***	0.390	**0.420***
SA	-0.021	-0.146	-0.182	**-0.393***	-0.157	0.018	0.291	-0.081	0.054

HOAs = higher-order aberrations; CCI = clear corneal incision; CCT = central corneal thickness; CV = corneal volume; CT-En = corneal thickness at incision entry; CT-Ex = corneal thickness at incision exit; IL = incision length; Angle-En = angle between incision and corneal epithelium; Angle-Ex = angle between incision and corneal endothelium; Dis-En = the distance from incision entry to central cornea; Dis-Ex = the distance from incision exit to central cornea; SA = spherical aberration

*Significant (P<.0025) after correction for multiple testing (n=324) based on false discovery rate (FDR)

Table 5 Correlation analysis between corneal HOAs (6 mm zone) and CCI features.

	CCT	CV	CT-En	CT-Ex	IL	Angle-En	Angle-Ex	Dis-En	Dis-Ex
Intact incision group									
Total cornea									
Total HOAs	-0.038	0.01	0.326	0.226	0.355	**-0.560***	-0.295	0.167	0.035
Vertical trefoil	-0.21	-0.374	**-0.478***	-0.244	**-0.441***	0.369	0.26	-0.067	0.065
Vertical coma	0.091	0.033	**-0.488***	**-0.422***	-0.062	**0.512***	0.199	**0.601***	**0.609***
Horizontal coma	-0.221	-0.181	-0.019	-0.383	0.221	-0.249	-0.114	-0.139	-0.156
Oblique trefoil	0.176	-0.228	-0.360	-0.042	-0.283	**0.420***	0.258	-0.128	0.054
SA	-0.331	**-0.440***	0	**-0.625***	-0.103	0.312	0.019	0.407	**0.435***
Anterior cornea									
Total HOAs	-0.05	-0.01	**0.444***	0.288	0.294	**-0.533***	-0.305	0.097	0.007
Vertical trefoil	-0.292	-0.309	0.007	-0.06	-0.361	**0.445***	0.373	0.083	0.236
Vertical coma	0.104	0.072	**-0.528***	-0.278	0.009	0.412	0.166	**0.532***	**0.515***
Horizontal coma	-0.218	-0.15	**-0.420***	**-0.461***	0.097	-0.264	-0.021	-0.168	-0.16
Oblique trefoil	-0.252	-0.252	-0.378	0.046	-0.271	**0.417***	0.27	-0.068	0.089
SA	-0.370	**-0.486***	0.014	**-0.602***	-0.099	0.372	0.012	0.366	0.406
Posterior cornea									
Total HOAs	0.251	0.195	-0.086	0.354	**0.494***	-0.355	-0.295	-0.373	-0.195
Vertical trefoil	-0.097	-0.042	-0.356	**-0.487***	-0.364	0.082	0.058	-0.261	-0.181
Vertical coma	0.018	-0.147	0.009	-0.395	-0.372	0.109	0.125	0.307	**0.416***
Horizontal coma	-0.006	-0.182	-0.219	-0.246	0.186	-0.319	-0.091	-0.058	-0.002
Oblique trefoil	**-0.595***	**-0.432***	-0.107	-0.368	-0.086	0.028	-0.007	-0.185	-0.09
SA	0.213	0.144	-0.098	-0.161	0.048	0.185	-0.093	0.138	0.063
Defective incision group									
Total cornea									
Total HOAs	-0.094	0.201	0.199	0.16	0.162	-0.22	-0.223	**-0.406***	-0.350
Vertical trefoil	0.063	0.094	0.053	0.016	**-0.433***	0.108	0.312	0.133	0.329

Vertical coma	-0.283	**-0.468***	**-0.409***	**-0.531***	-0.267	0.281	**0.390***	0.226	0.287
Horizontal coma	0.01	0.056	-0.194	0.142	**0.457***	-0.314	**-0.405***	0.071	-0.147
Oblique trefoil	-0.119	-0.282	-0.235	**-0.534***	-0.297	0.188	0.04	**0.402***	**0.389***
SA	-0.007	-0.144	-0.173	-0.164	0.013	0.235	0.318	0.233	0.14
Anterior cornea									
Total HOAs	-0.094	0.172	0.078	0.127	0.053	-0.206	-0.158	**-0.428***	-0.295
Vertical trefoil	0.062	0.128	0.197	0.133	**-0.364***	0.119	0.258	0.163	0.302
Vertical coma	-0.294	**-0.497***	**-0.407***	**-0.525***	-0.339	0.313	**0.437***	0.239	0.313
Horizontal coma	-0.029	0.033	-0.164	0.13	**0.399***	-0.297	**-0.365***	0.117	-0.076
Oblique trefoil	-0.154	-0.280	-0.17	**-0.498***	-0.295	0.204	0.156	**0.406***	**0.405***
SA	-0.041	0.13	-0.146	-0.089	0.021	0.249	0.278	0.325	0.217
Posterior cornea									
Total HOAs	0.124	0.323	0.128	0.21	**0.434***	-0.288	-0.282	**-0.384***	**-0.399***
Vertical trefoil	0.009	-0.049	-0.278	-0.209	-0.201	0.005	0.147	-0.053	0.093
Vertical coma	-0.03	-0.207	**-0.359***	**-0.386***	0.092	0.083	-0.001	0.343	**0.498***
Horizontal coma	0.157	0.148	-0.058	0.109	0.132	-0.203	-0.084	-0.204	-0.123
Oblique trefoil	0.116	-0.03	-0.138	-0.281	-0.321	-0.009	**0.413***	0.18	0.118
SA	0.09	-0.023	0.058	**-0.365***	0.042	-0.015	-0.188	**0.438***	0.292

HOAs = higher-order aberrations; CCI = clear corneal incision; CCT = central corneal thickness; CV = corneal volume; CT-En = corneal thickness at incision entry; CT-Ex = corneal thickness at incision exit; IL = incision length; Angle-En = angle between incision and corneal epithelium; Angle-Ex = angle between incision and corneal endothelium; Dis-En = the distance from incision entry to central cornea; Dis-Ex = the distance from incision exit to central cornea; SA = spherical aberration

*Significant (P<.0091) after correction for multiple testing (n=324) based on false discovery rate (FDR)

Table S1 Preoperative corneal HOAs data by CCI integrity.

Parameter	Intact incision (n=38)	Defective incision (n=54)
4 mm analytical zone		
Total cornea		
Total HOAs	0.217±0.104	0.200±0.090
Z(3, -3)	-0.044±0.112	-0.016±0.071
Z(3,-1)	0.078±0.097	0.032±0.121
Z(3,1)	0.018±0.066	-0.012±0.075
Z(3, 3)	-0.039±0.077	0.010±0.065
Z(4, -4)	0.019±0.047	0.011±0.047
Z(4, -2)	-0.012±0.027	0.001±0.023
Z(4, 0)	0.058±0.035	0.058±0.049
Z(4, 2)	-0.004±0.036	-0.017±0.044
Z(4, 4)	-0.010±0.052	-0.024±0.046
Anterior cornea		
Total HOAs	0.207±0.092	0.199±0.084
Z(3, -3)	-0.060±0.091	-0.015±0.061
Z(3,-1)	0.075±0.096	0.033±0.118
Z(3,1)	0.013±0.060	-0.011±0.077
Z(3, 3)	-0.017±0.066	0.012±0.058
Z(4, -4)	0.018±0.042	0.009±0.045
Z(4, -2)	-0.010±0.026	0.000±0.022
Z(4, 0)	0.069±0.035	0.072±0.044
Z(4, 2)	0.008±0.037	-0.009±0.045
Z(4, 4)	-0.001±0.046	-0.014±0.043
Posterior cornea		
Total HOAs	0.068±0.018	0.075±0.020
Z(3, -3)	-0.004±0.026	-0.001±0.039
Z(3,-1)	-0.010±0.027	-0.004±0.022
Z(3,1)	0.005±0.020	0.000±0.018
Z(3, 3)	-0.008±0.031	-0.002±0.031
Z(4, -4)	0.002±0.014	0.003±0.019
Z(4, -2)	-0.002±0.007	-0.002±0.012
Z(4, 0)	-0.031±0.012	-0.037±0.016
Z(4, 2)	-0.013±0.011	-0.009 ±0.011
Z(4, 4)	-0.010±0.013	-0.012±0.014
6 mm analytical zone		
Total cornea		
Total HOAs	0.691±0.237	0.654±0.211

Z(3, -3)	-0.230±0.228	-0.103±0.195
Z(3,-1)	0.198±0.255	0.094±0.279
Z(3,1)	0.038±0.135	-0.010±0.173
Z(3, 3)	-0.075±0.181	0.041±0.177
Z(4, -4)	0.005±0.132	0.013±0.108
Z(4, -2)	0.005±0.069	0.013±0.069
Z(4, 0)	0.403±0.110	0.396±0.149
Z(4, 2)	-0.044±0.107	-0.077±0.157
Z(4, 4)	-0.037±0.107	-0.064±0.089
Anterior cornea		
Total HOAs	0.676±0.211	0.673±0.211
Z(3, -3)	-0.213±0.238	-0.085±0.201
Z(3,-1)	0.165±0.248	0.078±0.280
Z(3,1)	0.043±0.129	-0.003±0.192
Z(3, 3)	-0.058±0.165	0.048±0.185
Z(4, -4)	-0.001±0.125	0.009±0.116
Z(4, -2)	0.008±0.067	0.013±0.064
Z(4, 0)	0.416±0.098	0.430±0.144
Z(4, 2)	-0.008±0.092	-0.060±0.138
Z(4, 4)	-0.016±0.092	-0.032±0.093
Posterior cornea		
Total HOAs	0.200±0.033	0.206±0.040
Z(3, -3)	-0.024±0.064	-0.022±0.079
Z(3,-1)	0.027±0.062	0.008±0.050
Z(3,1)	-0.003±0.045	-0.007±0.036
Z(3, 3)	-0.018±0.067	-0.007±0.045
Z(4, -4)	0.006±0.033	0.004±0.042
Z(4, -2)	-0.004±0.019	0.000±0.025
Z(4, 0)	-0.112±0.038	-0.132±0.036
Z(4, 2)	-0.040±0.030	-0.028±0.027
Z(4, 4)	-0.022±0.038	-0.034±0.042

HOAs = higher-order aberrations; CCI = clear corneal incision

Means ± SD

False discovery rate (FDR)-*P* >.05 for all the comparisons